Effect of the compression ratio on the performance and combustion of a natural-gas direct-injection engine

ARTICLE *in* PROCEEDINGS OF THE INSTITUTION OF MECHANICAL ENGINEERS PART D JOURNAL OF AUTOMOBILE ENGINEERING · JANUARY 2009

Impact Factor: 0.65 · DOI: 10.1243/09544070JAUTO976

Zuohua Huang
Xi'an Jiaotong University

Effect of the compression ratio on the performance and combustion of a natural-gas direct-injection engine

J-J Zheng, J-H Wang, B Wang, and **Z-H Huang***
State Key Laboratory of Multiphase Flow in Power Engineering, School of Energy and Power Engineering, Xi'an Jiaotong University, Xi'an, People's Republic of China

The manuscript was received on 23 July 2008 and was accepted after revision for publication on 16 September 2008.

DOI: 10.1243/09544070JAUTO976

Abstract: An experimental study on the combustion and emissions of a natural-gas direct-injection spark ignition engine under different compression ratios was carried out. The results show that the compression ratio has a large influence on the engine performance, combustion, and emissions. The penetration distance of the natural-gas jet is decreased and relatively strong mixture stratification is formed as the compression ratio is increased, giving a fast burning rate and a high thermal efficiency, especially at low and medium engine loads. However, the brake thermal efficiency is increased with a compression ratio up to a limit of 12 at high engine loads. The maximum cylinder gas pressure is increased with increase in the compression ratio. The flame development duration is decreased with increase in the compression ratio and this behaviour becomes more obvious with increase in the compression ratio at low loads or for lean mixture combustion. This indicates that the compression ratio has a significant influence on the combustion duration at lean combustion. The exhaust hydrocarbon (HC) and carbon monoxide emissions decreased with increase in the compression ratio, while the exhaust nitrogen oxide emission is increased with increase in the compression ratio. The exhaust HC emission tends to increase at high compression ratios. Experiments showed that a compression ratio of 12 is a reasonable value for a compressed-natural-gas direct-injection engine to obtain a better thermal efficiency without a large penalty of emissions.

Keywords: natural gas, compression ratio, direct injection, engine, combustion

1 INTRODUCTION

With increasing concern about fuel shortage and air pollution control, research on improving the engine fuel economy and reducing exhaust emissions has become the major topic in combustion and engine studies. Because of limited reserves of crude oil, the development of alternative-fuel engines has attracted more attention in the engine community. Alternative fuels usually are clean fuels compared with traditional diesel fuel and gasoline fuel in the engine combustion process. The introduction of these alternative fuels is beneficial to slowing down the fuel shortage and reducing engine exhaust emissions.

Natural gas is thought to be one of the most promising alternatives to traditional vehicle fuels for engines since it has cleaner combustion characteristics and plentiful reserves. Natural gas is widely used in taxis and city buses all over the world and the natural-gas-fuelled engine has been realized in both the spark ignition engine and the compression ignition engine. Furthermore, its high octane value and good anti-knock property permits a high compression ratio (CR) leading, of course, to higher thermal efficiency in the high-load condition. Previous studies showed low emissions by using natural gas. Engines fuelled with natural gas emit less carbon monoxide (CO) and non-methane hydrocarbons (HCs) compared with gasoline engines [**1**, **2**].

Nowadays, there are mainly two kinds of operating mode for engines fuelled with natural gas in actual

**Corresponding author: State Key Laboratory of Multiphase Flow in Power Engineering, School of Energy and Power Engineering, Xi'an Jiaotong University, Xi'an Ning West Road No. 28, Xi'an, 710049, People's Republic of China. email: zhhuang@mail.xjtu.edu.cn*

applications (or during routine operation). In the first operating mode, the homogeneous natural gas is ignited by pilot injection of the diesel fuel before the top dead centre (TDC). This needs two separate fuel systems and makes the system complicated. Meanwhile, HC emissions still remain high for light loads. In the second mode, the homogeneous mixture of natural gas and air is ignited by a spark plug as in the traditional homogeneous gasoline spark ignition engine. As natural gas occupies some fraction of intake charge, it has the disadvantage of low volumetric efficiency, and this decreases the amount of fresh air into the cylinder, leading to a decreased power output compared with that of a gasoline engine. The homogeneous charge combustion makes it difficult to burn the lean mixture. These engines have a lower thermal efficiency because engine knock is avoided and because of the unavoidable throttling at the intake for a partial load [**3**]. So-called homogeneous lean combustion engines have appeared. They can realize a higher thermal efficiency owing to the lower pumping loss, the lower heat loss, and the increase in the specific heat ratio, at the expense of the moderately higher nitrogen oxide (NO_x) emissions due to the ineffectiveness of the existing catalyst. The large cycle-by-cycle variation, however, restricts the lean operation limit of this type of homogeneous mixture engine [**4–8**].

In recent years, a gasoline direct-injection (GDI) engine has entered into the stage of production for modern two- and four-stroke petrol engines. The major advantages of a GDI engine are the increase in the fuel efficiency. The charge stratification formed by fuel injection and turbulence in the combustion chamber permits extremely lean combustion without high cycle-by-cycle variations, leading to a high combustion efficiency and low emissions at low loads [**9–11**]. In addition, there is no throttling loss in some GDI engines, which greatly improves the volumetric and thermal efficiencies in engines without a throttle valve. Moreover, the end gas mixture near the cylinder wall is very lean, reducing the occurrence of knocking, and this allows utilization of an increased CR to improve engine performance and thermal efficiency.

Direct-injection natural gas can be utilized to avoid the loss in volumetric efficiency, as natural gas is directly injected into the cylinder. It is flexible in mixture preparation because of forms a stratified mixture in the cylinder at low loads and improves the fuel economy. The ability to increase the CR can improve the engine performance. In addition, natural-gas direct-injection combustion can avoid smoke emission from GDI combustion [**12–15**]. Some previous studies were conducted on natural-gas direct-injection combustion by using a rapid compression machine and/or engines [**15–24**].

As has been clarified by previous studies [**25–30**], the CR is one of the most important factors for natural-gas engine operation because of its high anti-knock property. Increasing the CR can increase the thermal efficiency and power output; however, increasing the CR will also lead to high NO_x emissions especially at high engine loads. Thus, an optimum CR exists to obtain a high thermal efficiency without the penalty of high NO_x emissions. Kim *et al.* [**25**] investigated the performance of compressed natural gas (CNG) under two CRs in a modified gasoline–CNG dual-fuel engine. They found that, although the engine attained almost same power under both CRs, the exhaust total HC and NO_x emissions had higher values at higher CRs while the CO emission had a higher value at lower CRs. Yamin and Dado [**26**] carried out a numerical study on the performance of a four-stroke engine with variable stroke lengths and CRs. The results showed that the engine indicated power was increased as the CR was increased. Chaiyot [**27**] investigated the effect of the CR on the performance and emissions in a CNG dedicated engine by changing the pistons. The results showed that increasing the CR gave more power output. The NO_x emission showed a trend of first increasing and then decreasing with increase in the CR. Total HC emissions had a higher value when the CR increased, but the amount of CO emission on the average had higher values at lower CRs. Das and Watson [**28**] carried out an experimental investigation on a modified natural-gas engine at different CRs. The results showed that increasing the CR combined with cylinder turbulence enhancement allowed burning of lean mixtures without large cyclic variations. The engine with CR of 15.4 and multi-port injection could receive its best performances at maximum brake torque (MBT) ignition timings. High thermal efficiency and low HC emission were realized at the CR. In addition, high CRs also led to low carbon dioxide (CO_2) emission on increase in the thermal efficiency. Caton [**29**] studied the effect of the CR on NO_x emission in a spark ignition engine numerically from the thermodynamic cycle analysis and their study showed that the NO_x concentration had an increasing and then decreasing trend with the increase in the CR. The NO_x behaviour was also presented by Takagaki and Raine [**30**]. They found

a) Cross section view from the top

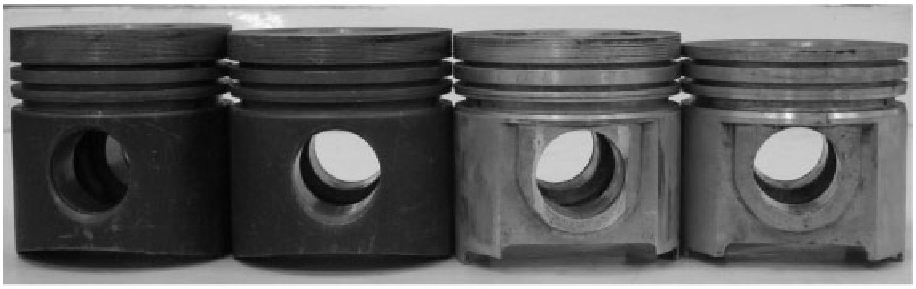

b) Cross section view from the front

Fig. 1 Pistons at different CRs (the pistons with CRs of 14, 12, 10, and 8 are arranged from left to right)

that, for fixed spark timing, NO_x emissions were increased on increase in the CR but, for maximum brake torque timing, NO_x emissions showed an increasing and then decreasing trend with increase in the CR. The variation in the NO_x emissions with increasing CR was explained by the combined effect of an increase in the burn rate and the kinetically controlled NO_x formation process.

As previous work reported only the effect of the CR on a homogeneous charge natural-gas engine, and few studies describing the effect of the CR on the natural-gas direct-engine have been conducted. Thus, this study is worthwhile. The objective is to investigate experimentally the effect of the CR on the combustion and engine performance in a natural-gas direct-injection engine in order to optimize the natural-gas direct-injection engine better.

2 EXPERIMENTAL SECTION

A single-cylinder modified natural-gas direct-injection spark ignition engine is used in this study [**14–16**]. The specifications of the engine are listed in Table 1.

In order to study the effect of the CR on the engine combustion and performance, four CRs obtained by modifying the piston crown were prepared. The images of the modified pistons are shown in Fig. 1 and the specifications of the pistons are listed in Table 2.

A production-type of gasoline swirl injector was used in the study. The flowrate of the injector under 8 MPa is 191.8 l/min. In addition to installing the natural-gas high-pressure injector, a spark plug was also installed into the centre of the combustion chamber as the ignition source and the experimental set-up and injector arrangement are shown in Fig. 2.

An electrical control system was used for engine operation and control. Injection timing, spark timing, and injection duration were controlled by the

Table 1 Engine specifications

Number of cylinders	1
Bore (mm)	100
Stroke (mm)	115
Length of the connecting rod (mm)	190
CR	8,10,12,14
Combustion chamber	Bowl-in-shape
Displacement (l)	0.903
Ignition source	Spark plug
Injection pressure (MPa)	8
Inlet valve opening	11° crank angle (CA) before top dead centre (BTDC)
Inlet valve closure	49° crank angle (CA) after bottom dead centre (ABDC)
Exhaust valve opening	52° crank angle (CA) before bottom dead centre (BBDC)
Exhaust valve closure	8° crank angle (CA) after top dead centre (ATDC)

Table 2 The specifications of the pistons

CR	Piston height (mm)	Top land height (mm)	Bore of piston cavity (mm)	Height of piston cavity (mm)
8	94.12	6.00	69.20	7.30
10	98.44	10.60	68.00	10.78
12	100.00	12.16	59.42	14.20
14	102.40	14.52	58.24	16.84

electronic control unit and could be regulated in the experiment.

The composition of natural gas used in this experiment is given in Table 3. Natural gas was prepared in advance in a CNG tank and was supplied to the fuel injector through a pressure regulator. Natural gas was injected into cylinder at a constant pressure of 8 MPa, since the gas velocity from the injector nozzle is kept at the constant value of the sonic velocity because of the condition of choke flow during fuel injection; thus the amount of injected fuel will maintain a constant value determined by the injection duration in the study.

The experiment were conducted at 70 per cent wide-open throttle and engine speeds of 1200 r/min and 1800 r/min. Six operation modes were conducted to study the effect of the CR, and the engine operating parameters are listed in Table 4. The experiments were conducted at fixed fuel injection timings and fixed ignition timings for the same mode. Thus, the influence of the CR on natural-gas direct-injection combustion can be attributed to the influence from varying the CR.

3 INSTRUMENTATION AND METHOD OF CALCULATION

A Horiba MEXA-554J analyser and a Horiba MEXA-720NOx gas analyser were used to measure exhaust HC, CO, CO_2, and NO_x concentrations, and the analysers have the measuring accuracy of 1 ppm for HC, 0.01 per cent for CO, 0.01 per cent for CO_2, and 1 ppm for NO_x. The MEXA-720 NO_x analyser was calibrated using nitrogen N_2 and nitric oxide (NO)–N_2 calibration gases when a CR was changed and the MEXA-554J analyser was recalibrated using propane (C_3H_8), hydrogen (H_2), CO, etc. Calibration was carried out each time that the analyser power was turned on. In the experiments, the exhaust gases

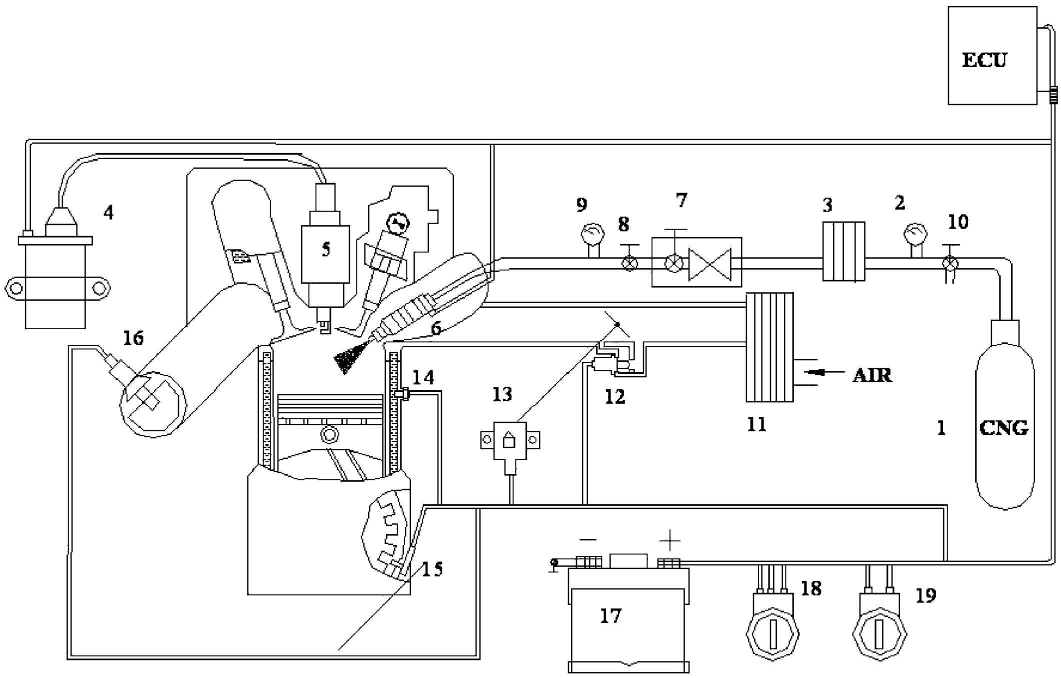

Fig. 2 Experimental set-up and injector arrangement: 1, CNG bomb; 2, pressure gauge (40 MPa); 3, fuel filter; 4, high-pressure coil; 5, spark plug; 6, CNG injector; 7, pressure-releasing valve; 8, protecting valve; 9, pressure gauge (20 MPa); 10, CNG feeding valve; 11, air filter; 12, idling speed control motor; 13, throttle valve position sensor; 14, coolant temperature sensor; 15, speed sensor; 16, oxygen sensor; 17, battery; 18, ignition switch; 19, CNG switch; ECU, electronic control unit

Table 3 Composition of natural gas

Gas	Amount (vol %)
CH_4	96.16
$i\text{-}C_4H_{10}$	0.021
$n\text{-}C_5H_{12}$	0.005
H_2S	0.0002
C_2H_6	1.096
$n\text{-}C_4H_{10}$	0.021
N_2	0.001
H_2O	0.006
C_3H_8	0.136
$i\text{-}C_5H_{12}$	0.006
CO_2	2.54

were measured when the engine operating parameters were adjusted to the specified conditions, i.e. exhaust gases were measured at steady operating conditions. In this study, fuel consumption is measured using the weighting method and the thermal efficiency is calculated from the fuel consumption and engine torque.

The cylinder pressure was recorded with a piezoelectric transducer (type 6117BFD17) made by Kistler (installed into the cylinder) with a resolution of 10 Pa, and the dynamic TDC was determined by motoring. The CA signal was obtained from a Kistler angle-generating device (CA encoder type 2613B) mounted on the main shaft, while information on the pressure and CA was recorded with a Yokogawa data acquisition system DL750. The signal of the cylinder pressure was acquired for every 0.1° CA, and the acquisition process covered 100 completed cycles. The average value of these 100 cycles was output as the pressure data used to calculate the heat release and combustion parameters.

A thermodynamic model based on the homogeneous cylinder content assumption is used to calculate the thermodynamic parameters in this paper. The model neglects the leakage through the piston rings [**31**], and thus the energy conservation in the cylinder is written as

$$\frac{dQ_B}{d\theta} = mT\frac{dC_V}{d\theta} + p\frac{C_p}{R}\frac{dV}{d\theta} + \frac{C_V V}{R}\frac{dp}{d\theta} + \frac{dQ_W}{d\theta} \tag{1}$$

where the heat transfer rate is given by

$$\frac{dQ_W}{d\theta} = h_c A(T - T_w) \tag{2}$$

The heat transfer coefficient h_c uses the correlation formula given by Woschni [**32**].

Properties such as the constant-pressure heat capacity and the constant-volume heat capacity for species are obtained from the NASA database [**33**, **34**]. Because the mass fraction burned is unknown at every time step, a simple iterative method is introduced to calculate the thermodynamic properties of the mixture, which includes burned and unburned parts.

The primary sources are cylinder pressure data. Using those primary data and the above formula, the heat release rate, the peak pressure, the mean gas temperature, and the maximum mean gas temperature can be calculated.

The flame development duration is defined as the interval of CA from the ignition start to that of 10 per cent mass fraction burned duration; the rapid combustion duration is defined as the interval of CA from 10 per cent mass fraction burned duration to 90 per cent mass fraction burned duration; the total combustion duration is the duration of the overall burning process and it is the sum of flame development duration and rapid combustion duration.

The CA of the centre of the heat release curve is determined from the formula

$$\theta_c = \frac{\int_{\theta_s}^{\theta_e} (dQ_B/d\theta)\theta\, d\theta}{\int_{\theta_s}^{\theta_e} (dQ_B/d\theta) d\theta} \tag{3}$$

in which θ_s is the CA at the beginning of heat release and θ_e is the CA at the end of heat release.

4 RESULTS AND DISCUSSION

The brake thermal efficiency η versus the CR for various brake mean effective pressures (bmeps) are shown in Fig. 3. The brake thermal efficiency

Table 4 Engine operating parameters

Operating mode	n_e (r/min)	p_{me} (MPa)	θ_{inj} (deg CA BTDC)	θ_{ign} (deg CA BTDC)	Δt_{injd}(ms) for the following CRs				λ for the following CRs			
					8	10	12	14	8	10	12	14
1	1200	0.14	150	20	14.46	12.42	11.22	10.92	1.409	1.494	1.583	1.845
2	1200	0.42	168	24	14.76	14.72	12.82	12.46	1.238	1.385	1.410	1.601
3	1200	0.70	180	30	18.26	17.72	16.62	17.06	1.034	1.168	1.214	1.190
4	1800	0.14	180	27	15.96	13.82	13.22	12.56	1.470	1.528	1.723	2.068
5	1800	0.42	190	32	16.66	14.92	14.19	12.96	1.292	1.335	1.535	1.608
6	1800	0.70	210	34	18.26	18.02	15.89	15.46	1.012	1.055	1.168	1.048

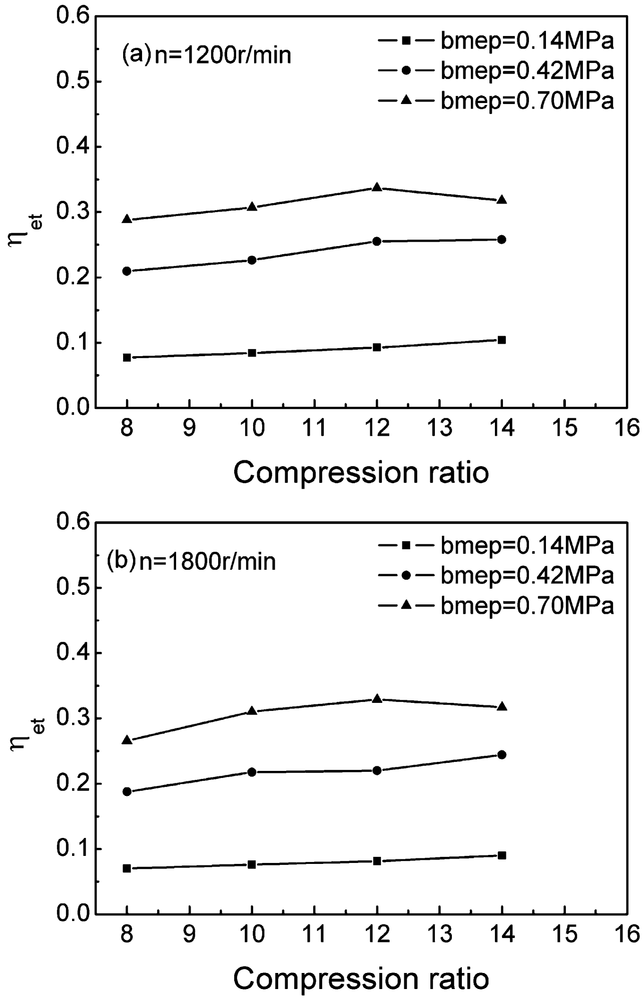

Fig. 3 Brake thermal efficiency versus CR

increases with increase in the CR at low and medium engine loads. However, the brake thermal efficiency is increased with increasing CR up to a limit of 12 at high engine loads.

The following reasons are considered to influence the brake thermal efficiency from the variation in the CR.

1. Increasing the CR will increase the cylinder gas pressure, temperature, and mixture concentration at the end of the compression stroke. This speeds up the chemical reactions, resulting in increases in the burning rate and the thermal efficiency.
2. The expansion ratio is increased with increase in the CR, and this decreases the exhaust gas temperature and reduces the energy carried away by the exhaust gases, leading to an increase in the thermal efficiency.
3. Increasing the CR increases the cylinder gas temperature at the end of the compression stroke and decreases the exhaust gas temperature during the late expansion and exhaust stroke. This will extend the temperature difference between high-temperature and low-temperature cycles, resulting in an increase in thermal efficiency [**31**].
4. With increasing CR, the clearance volume is decreased. The reduction in the clearance volume also improves the combustion, resulting in an increase in the flame temperature, which will increase the thermal efficiency.
5. Increasing the CR increases the surface-to-volume ratio of the combustion chamber at TDC, which should increase the heat transfer rates and heat loss. This will decrease the thermal efficiency.
6. Increasing the CR will also decrease the jet penetration distance and increase the jet cone angle [**35**] owing to an increased back pressure in cylinder. Thus, more injected fuel will concentrate on the local region near the centre part of the cylinder and form a locally rich stratified mixture in the cylinder. This will favour flame development under a relatively lean mixture, increasing the combustion rate and thermal efficiency. However, if too much fuel is concentrated on the local region near the centre part of cylinder (large CR under high-load operation), an over-stratified mixture will be formed, and utilization of the cylinder air is decreased. This will be unfavourable to mixture preparation and combustion, resulting in a decrease in the combustion rate and brake thermal efficiency. The influence of the CR on fuel jet stratification is evidence by the large difference between the stratified charge combustion and the homogeneous charge combustion [**27**, **30**].
7. In addition, the strength of squish is increased with increase in the CR, leading to increases in the turbulence intensity and flame propagation speed. Fast and short combustion duration occurs with increase in the CR, leading to an increase in the thermal efficiency.

The influence of point (5) is relatively less than those of points (1), (2), (3), (4), (6), and (7) for the relatively lean mixture combustion; thus the brake thermal efficiency increases with increase in the CR at low and medium engine loads as well as lower CRs (less than 12) under high engine loads, In contrast with this, the influence of points (5) and (6) becomes dominant factors under higher CRs (greater than 12) and high engine loads; therefore, the brake thermal efficiency increases as the CR becomes larger than 12 at high engine loads.

For a specific CR, the brake thermal efficiency increases with increase in the engine load. In natural-gas direct-injection combustion, the overall excess air ratios are larger than 1.0. Increasing the engine load increases the amount of fuel injected and decreases the overall excess air ratio. On the one hand, as the strong stratified mixture becomes richer overall, which increases the local mixture strength, the burning velocity can increase and the heat release process shorten. On the other hand, the richer mixture will reduce the thermodynamic efficiency of the mixture, which is unfavourable to the thermal efficiency, but the influence is relatively poor for an overall relatively lean mixture. The combined influence leads to an increase in the thermal efficiency as the engine load increases.

Figure 4 illustrates the flame development duration versus the CR for natural-gas direct-injection combustion. The flame development duration is decreased with increase in the CR. This can be regarded as improvement in the ignitibility and fast flame development under a higher unburned gas temperature at higher CRs. Moreover, the stratified mixture will increase the burning velocity and high turbulence is presented at high CRs. All these contribute to a decrease in the flame development duration as the CR is increased. In addition to these, the decrease in the residual gases as the CR is increased can decrease the influence of mixture dilution from the residual gases, and this can also promote flame development at the early stage of flame propagation.

The effect of increasing the CR on the flame development duration will become more obvious at low loads. Mixture stratification has a greater effectiveness on shortening the flame development duration at large excess air ratios or for lean mixture combustion. Lean mixture combustion usually has a low flame propagation speed; mixture stratification can accelerate the flame propagation speed. An increase in the CR will enhance the mixture

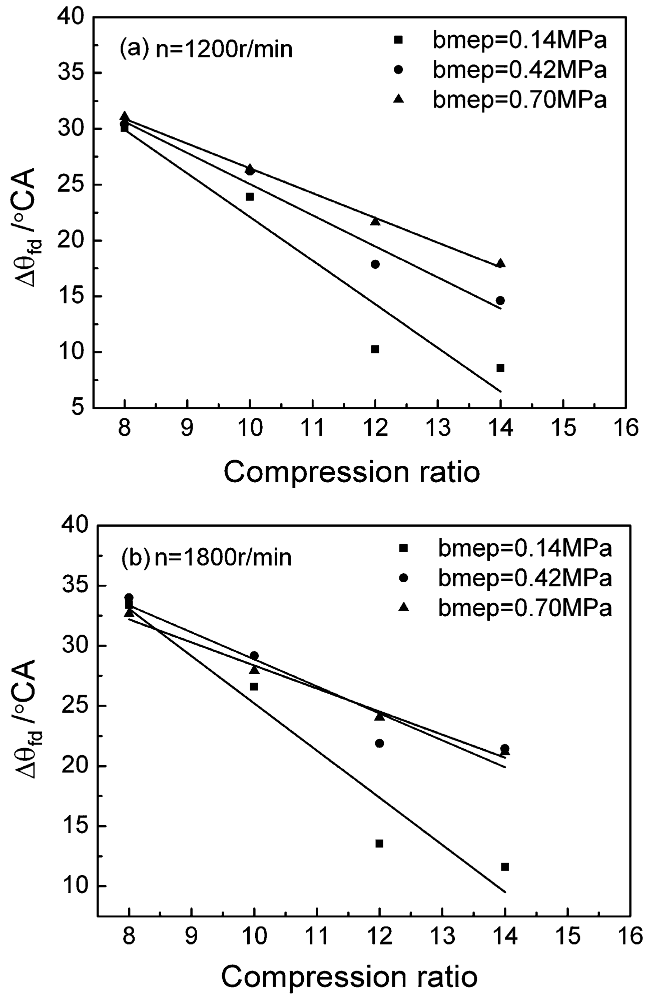

Fig. 4 Flame development duration versus CR

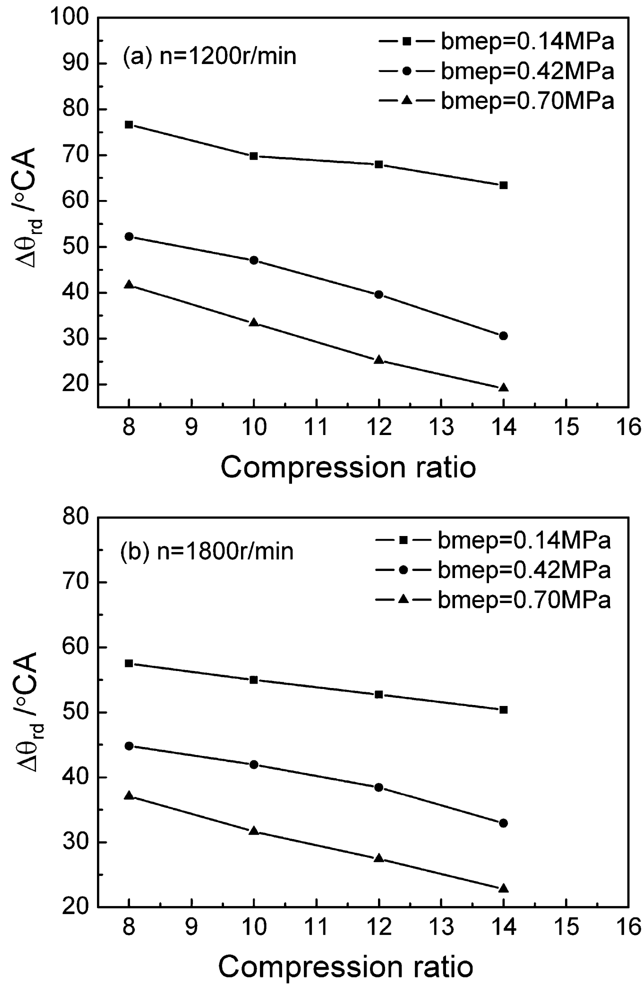

Fig. 5 Rapid combustion duration versus CR

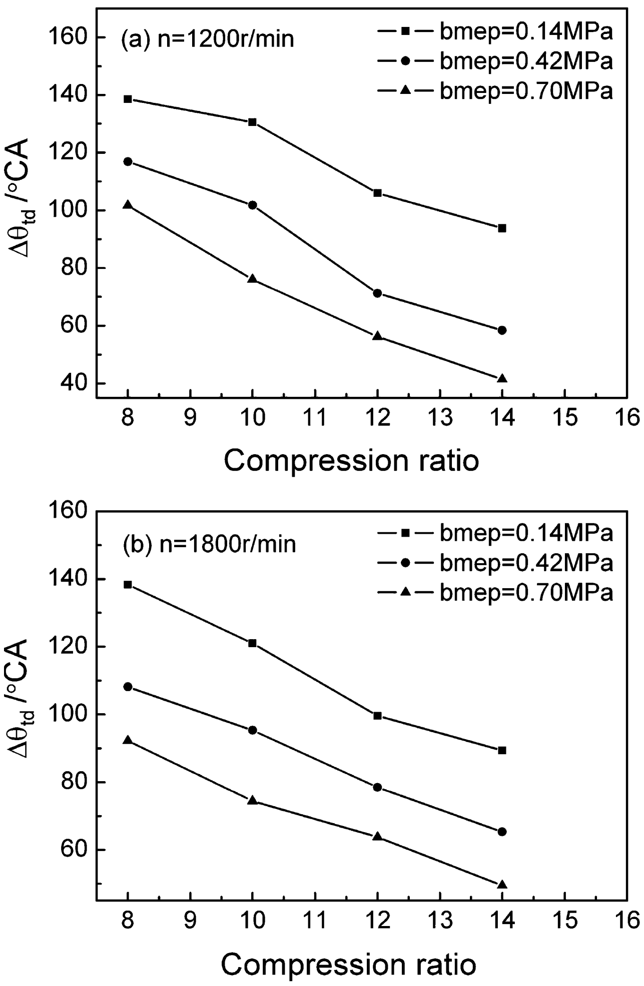

Fig. 6 Total combustion duration versus CR

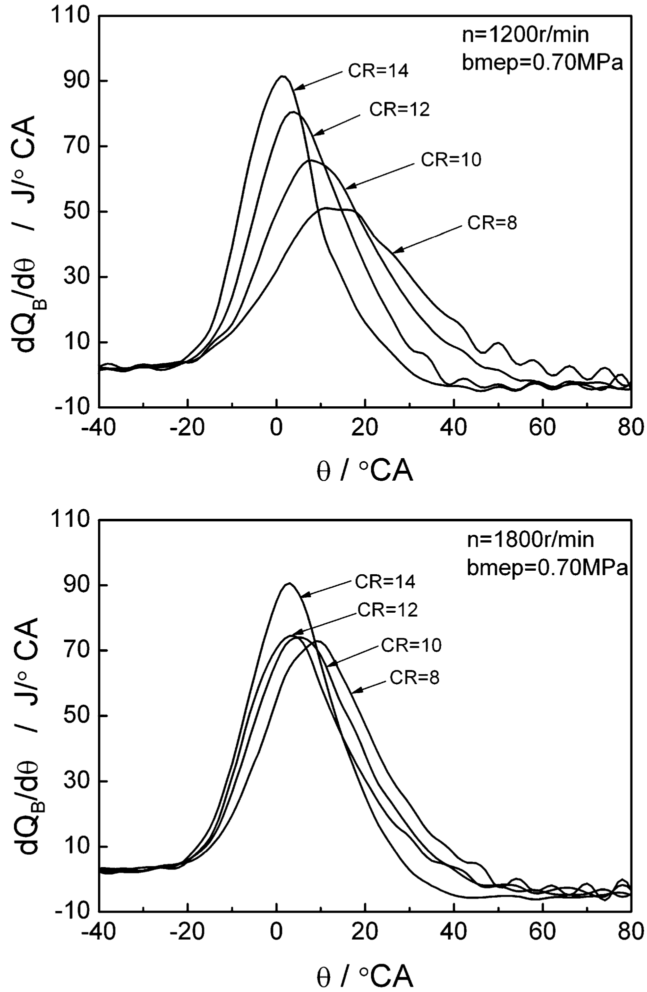

Fig. 7 Heat release rate of the fuel at a bmep of 0.70 MPa

stratification at low loads and results in a short flame development duration.

Figure 5 shows the rapid combustion duration versus the CR. Similar to the variation in the flame development duration with the CR, the rapid combustion duration also shows a decreasing trend with increase in the CR, and this suggests compactness of the heat release process with increasing CR. The increase in the unburned gas temperature and turbulence as well as mixture stratification contribute to the decrease in the rapid combustion duration on increasing the CR. Similarly, the decrease in the residual gas fraction on increasing the CR also increases the flame propagation speed.

Figure 6 gives the total combustion duration versus the CR. The total combustion duration decreased with increase in the CR. This is reasonable because both flame development duration and rapid combustion duration decreased on increasing the CR.

Figure 7 gives the heat release rate curves at bmep = 0.70 MPa versus the CR. The beginning of heat release is advanced on increasing the CR and the maximum heat release rate is increased with increase in the CR. This phenomenon is more obvious at low engine speeds, as the enhancement of burning velocity is more obvious with increasing CR, and this makes the phase of maximum heat release move close to the top dead centre and increases the thermal efficiency. The effect of the CR on the maximum heat release rate enhancement gives a limited value when $CR < 12$ while the maximum heat release rate increases markedly when $CR > 12$ as the heat transfer rates and heat loss increase with increasing CR and the effect is more obvious at large CRs and high loads. This is consistent with the behaviour of the thermal efficiency improvement on increasing the CR.

Figure 8 gives the CA θ_c of the centre of heat release curve relative to the TDC versus the CR. The CA θ_c of the centre of the heat release curve reflects the heat release compactness that is used as a parameter

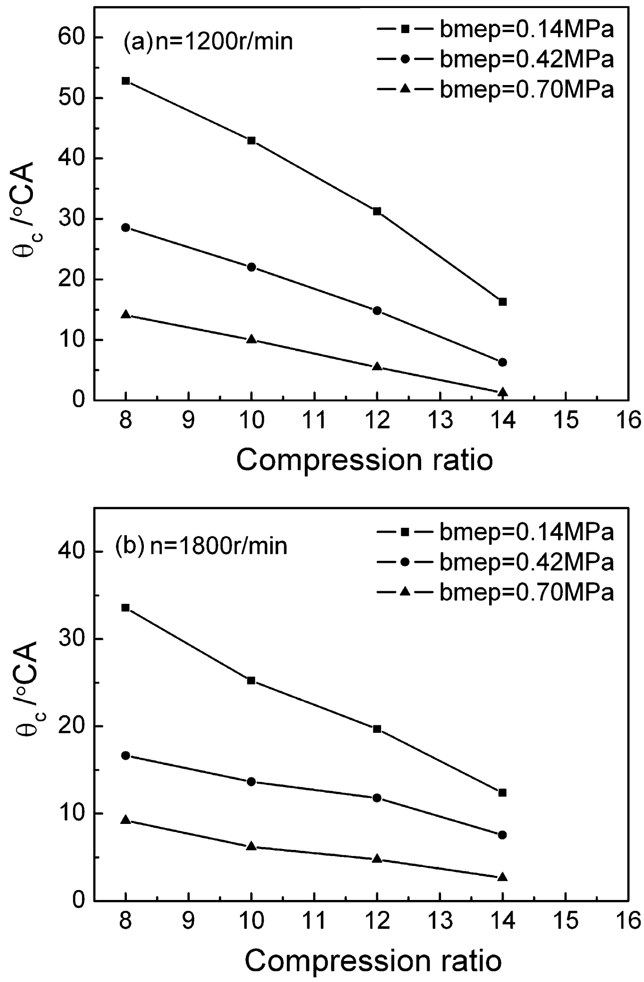

Fig. 8 CA of the centre of the heat release rate curve versus CR

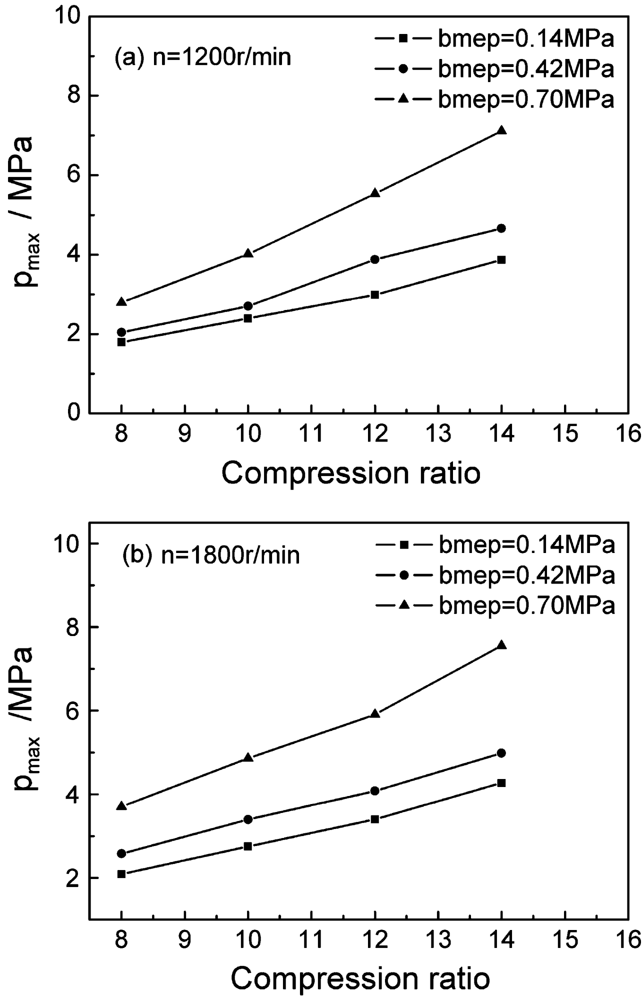

Fig. 9 Maximum cylinder gas pressure versus CR

for indicating combustion compactness because the spark timings are fixed at the same engine speed and load. The figure shows that θ_c tends to a small value on increasing the CR, and this suggests compactness of the heat release process on increasing the CR again. The increase in flame propagation speed contributes to this phenomenon, and this is consistent with the behaviour of the thermal efficiency improvement on increasing the CR.

Figure 9 shows the maximum cylinder pressure versus the CR. The maximum cylinder pressure increases with increasing CR. Two reasons are responsible for this behaviour. One is the rises in the unburned gas temperature and pressure with increasing CR. The other is the compact heat release process on increasing the CR. Both factors favour an increase in the maximum cylinder pressure.

Figure 10 shows the maximum mean gas temperature calculated from the thermodynamic model versus the CR. Similar to the behaviour of the maximum cylinder pressure, the maximum mean gas temperature also presents an increasing trend on increasing the CR. This is reasonable since the temperature at the moment of ignition increases with increasing CR. The increase in the burning velocity with increasing CR will also contribute to the increase in the maximum cylinder gas temperature. The results support the fact that the heat transfer increases with increasing CR since the engine will undergo higher heat transfer at higher gas temperatures.

Figure 11 gives the exhaust NO_x concentration versus the CR. At low and middle engine loads, the NO_x concentration has a low value and it does not vary on increasing the CR. The lean mixture combustion results in this behaviour. However, at high engine loads, the NO_x concentration shows an increasing trend with increasing CR. An almost linear increase in the NO_x emissions is observed with increasing CR at high engine loads. The

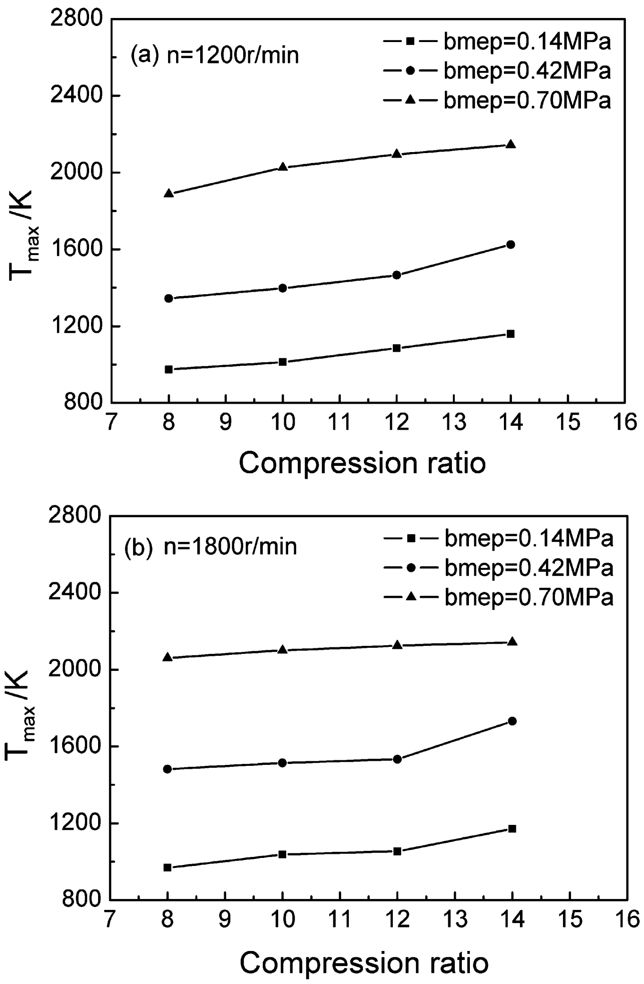

Fig. 10 Maximum mean gas temperature versus CR

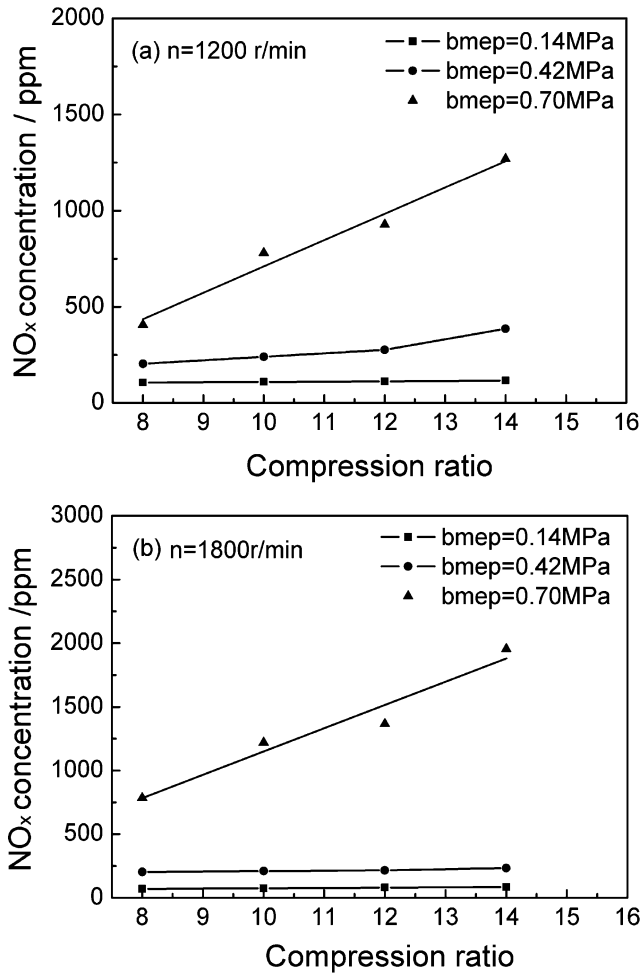

Fig. 11 Exhaust NO_x concentration versus CR

relatively high burning rate of the overall rich mixture combustion and a high-temperature environment contribute to the increase in the NO_x emissions with increasing CR at high engine loads. The trend of NO_x emissions is different from that of the homogeneous charge case [**30**]. The NO_x concentration increases with increase in the CR at fixed ignition timings and NO_x emissions show an increasing trend and then a decreasing trend for MBT timing.

Top-land crevice is one of the major sources for unburned HC emissions [**31**]. Figure 12 shows the HC emission versus the CR. For a specific engine load, HC emissions show a decreasing trend with increasing CR from 8 to approximately 12 and then an increasing trend on further increasing the CR from approximately 12 to 14. When the CR is increased, the jet penetration decreases. This will reduce the injected fuel entering into the top-land crevice region and reduce the HC emission with increasing CR. However, further increasing the CR will lead to a more stratified mixture in the cylinder and increase the rich mixture region in the cylinder; the lack of oxygen in this rich mixture region will bring more unburned HCs. Meanwhile, the low gas temperature at the expansion and exhaust strokes with increasing CR will decrease the HC oxidation in the expansion and exhaust processes. These two factors lead to an increase in the HC concentration when further increasing the CR. The trend of the HC emissions is also different from the homogeneous charge case [**30**], for the HC concentration increases with increase in the CR at fixed ignition timings, and HC emissions show an increasing trend and then a decreasing trend for MBT timings.

Figure 13 shows the CO concentration versus the CR. The CO concentration decreases with increasing CR for the stratified charge engine. Volumetric efficiency is increased and residual gas fraction is decreased with increasing CR. Thus, more fresh air and less dilution are present on increasing the CR. As CO is mainly dependent on the air-to-fuel ratio, the

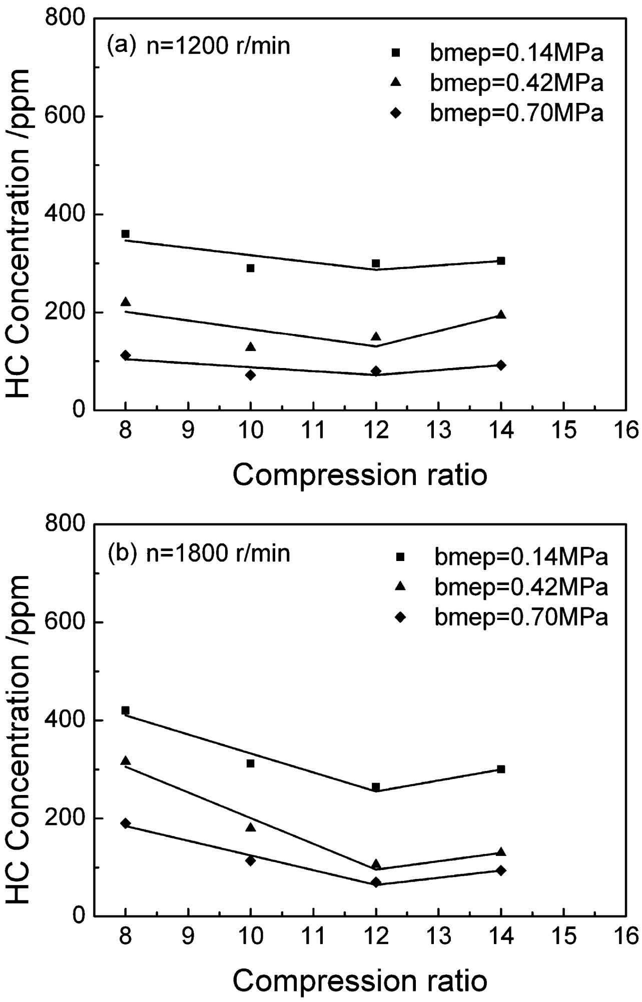

Fig. 12 Exhaust HC concentration versus CR

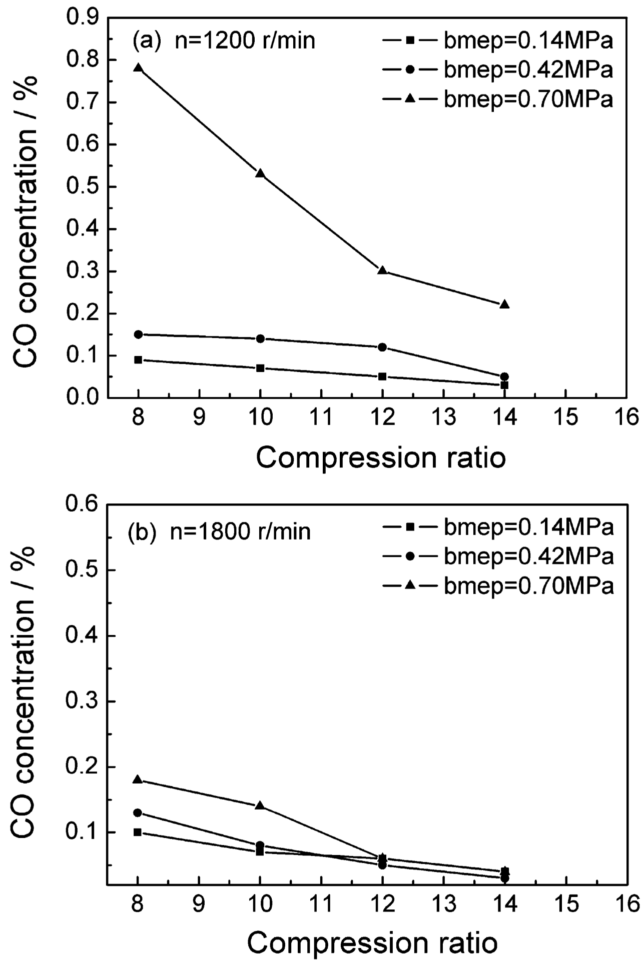

Fig. 13 Exhaust CO concentration versus CR

increase in the air-to-fuel ratio will cause low CO emission. The excess air ratio is relatively larger at the low and medium loads (the overall equivalence ratio is about 0.6–0.7), and the CO formed could be oxidized further under these conditions. Therefore, the CO concentration has a low value and it is slightly influenced by the CR. However, the local equivalence ratio may exceed 1.0 at high loads (the overall equivalence ratio is about 0.9), which leads to the production of larger amounts of CO, and increasing the CR can markedly increase the fresh air and decrease CO emission.

From the results above, it can be seen that the brake thermal efficiency of the natual-gas direct-injection engine increases with increase in the compression ratio, but the NO_x emissions also increase with increase in the CR, and this is the main problem facing the natual-gas direct-injection engine after increasing the CR. Thus, a compromise CR should be selected to obtain benefits from both performance and NO_x emissions.

Figure 14 gives the brake thermal efficiency and NO_x concentration at different CRs. The study shows that a CR of 12 will provide a good thermal efficiency without markedly increasing the NO_x emissions. At a CR of 14, the brake thermal efficiency tends to decrease with markedly high NO_x levels. Thus, further increasing the CR causes both the thermal efficiency and the NO_x level to deteriorate. Based on the experimental results, the optimum CR for the natural-gas direct-injection engine is 12.

5 CONCLUSIONS

The effect of the CR on engine performance and combustion was studied in a natural-gas direct-injection engine. The main conclusions are summarized as follows.

1. The CR has a large influence on the engine performance, combustion, and emissions. The

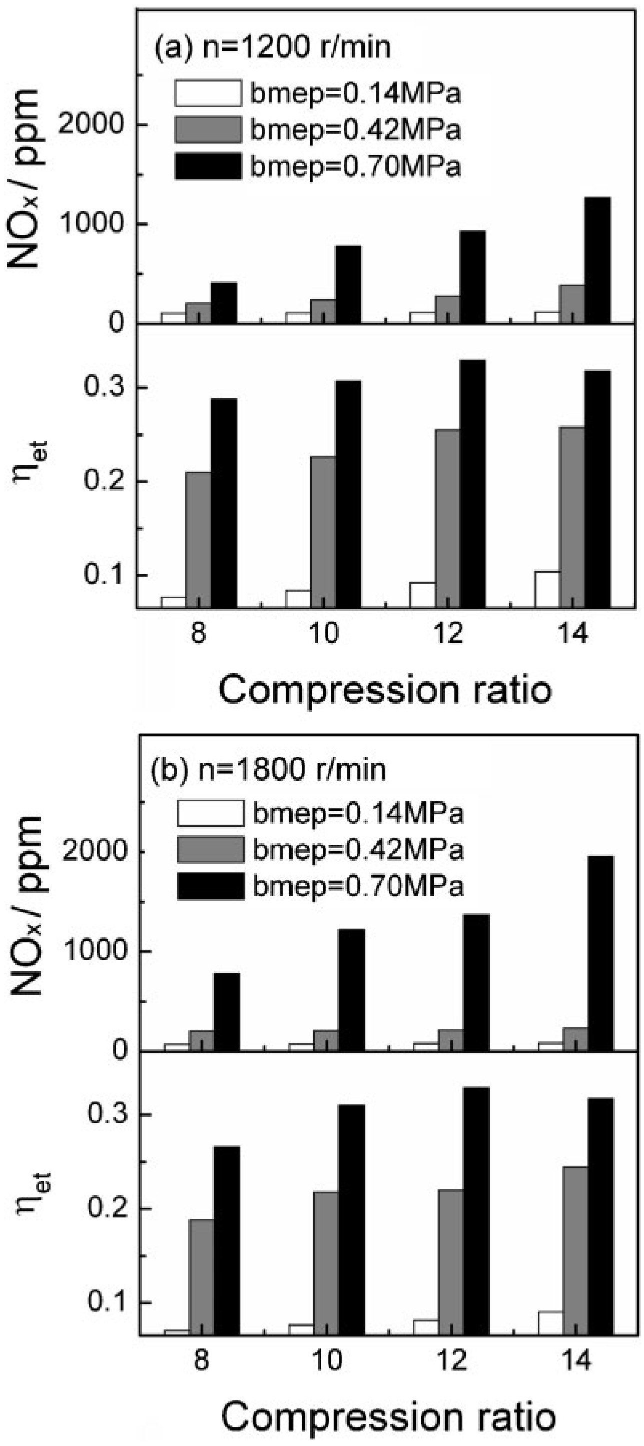

Fig. 14 Brake thermal efficiency versus exhaust NO_x concentration for various CRs

brake thermal efficiency increases with increase in the CR at low and medium engine loads, but the brake thermal efficiency increases with increasing CR up to a limit of 12 at high engine loads, and this is different from the homogeneous charge case.

2. The maximum cylinder gas pressure and the maximum gas mean temperature increase on increasing the CR. The flame development duration, the rapid combustion duration, and the total combustion duration decrease on increasing the CR.
3. Exhaust CO decreases while NO_x increases with increasing CR. The HC concentration shows a decreasing trend and then an increasing trend with increasing CR. The trends of NO_x and HC emissions with increasing CR are different from the results in previous literature for the homogeneous charge condition.
4. Based on the comprehensive evaluation of engine performance and emissions, a CR of 12 is suggested as the optimum value for the natural-gas direct-injection engine.

ACKNOWLEDGEMENTS

This study was supported by the National Natural Science Foundation of China (Grant 50636040), and the National Basic Research Program of China (Grant 2007CB210006).

REFERENCES

1 **Weaver, C. S.** Natural gas vehicles – a review of the state of the art. SAE paper 892133, 1989.
2 **Rousseau, S., Lemoult, B.,** and **Tazerout, M.** Combustion characteristics of natural gas in a lean burn spark-ignition engine. *Proc. Instn Mech. Engrs, Part D: J. Automobile Engineering*, 1999, **213**(5), 481–489.
3 **Yamamoto, Y., Sato, K.,** and **Matsumoto, S.** Study of combustion characteristics of compressed natural gas as automotive fuel. SAE paper 940761, 1994.
4 **Ben, L., Dacros, N. R., Truquet, R.,** and **Charnay, G.** Influence of air/fuel ratio on cyclic Variation and exhaust emission in natural gas SI engine. SAE paper 992901, 1999.
5 **Hassaneen, A. E., Varde, K. S., Bawady, A. H.,** and **Morgan, A. A.** A study of the flame development and rapid burn durations in a lean-burn fuel injected natural gas S.I. engine. SAE paper 981384, 1998.
6 **Ramesh, A., Corre, O.,** and **Tazerout, M.** Experimental investigation on cycle by cycle variations in a natural gas fulled spark ignition engine. In Proceedings of the Second International SAE India Mobility Conference, Chennai, India, 10–12 January 2002, pp. 145–152 (SAE International, Univerdale, Pennsylvania).

7 **Choa, H. M.** and **He, B. Q.** Spark ignition natural gas engines – a review. *Energy Conversion Mgmt*, 2007, **48**(2), 608–618.

8 **Corbo, P., Gambino, M., Iannaccone, S.,** and **Unich, A.** Comparison between lean-burn and stoichiometric technologies for CNG heavy-duty engines. SAE paper 950057, 1995.

9 **Brehob, D. D., Stein, R. A.,** and **Haghgooie, M.** Stratified-charge engine fuel economy and emission characteristics. SAE paper 982704, 1998.

10 **Kano, M., Saito, K.,** and **Basaki, M.** Emissions and fuel economy of a 1998 Toyota with a direct injection spark ignition engine. SAE paper 981462, 1998.

11 **Iwamoto, Y., Noma, K., Nakayama, O., Yamauchi, T.,** and **Ando, H.** Development of gasoline direct injection engine. SAE paper 970541, 1997.

12 **Willi, M. L.** and **Richards, B. G.** Design and development of a direct injected, glow plug ignition-assisted, natural gas engine. *Trans. ASME, J. Engng Gas Turbines Power*, 1995, **117**(4), 799–803.

13 **Meyers, D. P., Bourn, G. D., Hedrick, J. C.,** and **Kubesh, J. T.** Evaluation of six natural gas combustion systems for LNG locomotive applications. SAE paper 972967, 1997.

14 **Huang, Z. H., Wang, J. H., Liu, B., Zeng, K., Yu, J. R.,** and **Jiang, D. M.** Combustion characteristics of a direct-injection engine fueled with natural gas–hydrogen mixtures. *Energy Fuels*, 2006, **20**(2), 540–546.

15 **Zeng, K., Huang, Z. H., Liu, B., Liu, L. X., Jiang, D. M., Ren, Y.,** and **Wang, J. H.** Combustion characteristics of a direct-injection natural gas engine under various injection timings. *Appl. Thermal Engng*, 2006, **26**(8–9), 806–813.

16 **Liu, L. X., Huang, Z. H., Jiang, D. M., Ren, Y.,** and **Wang, Q.** Study on cycle-by-cycle variations in a direct injection natural gas engine (in Chinese). *Trans. CSICE*, 2005, **23**(1), 18–27.

17 **Honjo, F., Miura, A., Nakamura, A.,** and **Tsuchiya, T.** CNG in-cylinder direct injection engine system. In Proceedings of the JSAE Annual Congress, 2004, vol. 118(04), pp. 13–16 (Society of Automotive Engineers of Japan, Tokyo).

18 **Yuichi, G.** Mixture formation and ignition in a direct injection natural gas engine. *JSME Int. J., Ser. B*, 1999, **42**(2), 268–274.

19 **Hill, P. G.** and **Douville, B.** Analysis of combustion in diesel engines fueled by directly injected natural gas. *Trans. ASME, J. Engng Gas Turbines Power*, 2000, **112**(1), 141–149.

20 **Douville, B., Ouellette, P., Touchette, A.,** and **Ursu, B.** Performance and emissions of a two-stroke engine fueled using high-pressure direct injection of natural gas. *SAE Trans.*, 1998, **107**(3), 1727–1735.

21 **Huang, Z. H., Shiga, S., Ueda, T., Jingu, N., Nakamura, H., Ishima, T., Obokata, T., Tsue, M.,** and **Kono, M.** A basic behavior of CNG DI combustion in a spark-ignited rapid compression machine. *JSME Int. J., Ser. B*, 2002, **45**, 891–900.

22 **Huang, Z., Shiga, S., Ueda, T., Nakamura, H., Ishima, T., Obokata, T., Tsue, M.,** and **Kono, M.** Combustion characteristics of natural-gas direct-injection combustion under various fuel injection timings. *Proc. Instn Mech. Engrs, Part D: J. Automobile Engineering*, 2003, **217**(5), 393–401.

23 **Huang, Z., Shiga, S.,** and **Ueda, T.** Effect of fuel injection timing relative to ignition timing on the natural-gas direct-injection combustion. *Trans. ASME, J. Engng Gas Turbines Power*, 2003, **125**(3), 783–790.

24 **Huang, Z., Shiga, S., Ueda, T., Nakamura, H., Ishima, T., Obokata, T., Tsue, M.,** and **Kono, M.** Study of cycle-by-cycle variations of natural gas direct injection combustion using a rapid compression machine. *Proc. Instn Mech. Engrs, Part D: J. Automobile Engineering*, 2003, **217**(1), 53–62.

25 **Kim, B. S., Lee, Y. J.,** and **Koh, C. J.** Performance characteristic of CNG vehicle at various compression ratio. *Energy Engng*, 1996, **5**(1), 42–49.

26 **Yamin, J. A. A.** and **Dado, M. H.** Performance simulation of a four stroke engine with variable stroke-length and compression ratio. *Appl. Energy*, 2004, **77**(4), 447–463.

27 **Chaiyot, D.** *An experiment study on influence of compression ratio for performance and emission of natural gas retrofit engine.* MS Thesis, Department of Mechanical Engineering, Faculty of Engineering, Thai–German Graduate School, King Mongkut's Institute of Technology North Bangkok, 2006.

28 **Das, A.** and **Watson, H. C.** Development of a natural gas spark ignition engine for optimum performance. *Proc. Instn Mech. Engrs, Part D: J. Automobile Engineering*, 1997, **211**(5), 361–378.

29 **Caton, J. A.** Effect of the compression ratio on nitric oxide emissions for a spark ignition engine: results from a thermodynamic cycle simulation. *Int. J. Engine Res.*, 2003, **4**(4), 249–268.

30 **Takagaki, S. S.** and **Raine, R. R.** The effects of compression ratio on nitric oxide and hydrocarbon emissions from a spark-ignition natural gas fuelled engine. SAE paper 970506, 1997.

31 **Heywood, J. B.** *Internal combustion engine fundamentals*, 1988 (McGraw-Hill, New York).

32 **Woschni, G.** Universally applicable equation of the instantaneous heat transfer coefficient in the internal combustion engine. SAE paper 670931, 1967.

33 **McBride, B. J.** and **Gordon, S.** Computer program for calculation of complex chemical equilibrium compositions and applications. I. Analysis, NASA Reference Publication 1311, National Aeronautics and Space Administration, October 1994.

34 **McBride, B. J.** and **Gordon, S.** Computer program for calculation of complex chemical equilibrium compositions and applications. II. User's manual and program description. NASA Reference Publication 1311 National Aeronautics and Space Administration, June 1996.

35 **An, B., Narusawa, K.,** and **Sato, Y.** Analysis and visualization of compressed natural gas jet under

high-temperature and high-pressure conditions. *JSAE Trans.*, 2004, **35**(1), 33–38.

APPENDIX

Notation

A	wall area (m^2)
BTDC	before top dead centre
C_p	constant pressure specific heat (kJ/kg K)
C_V	constant volume specific heat (kJ/kg K)
$dp/d\theta$	rate of pressure rise with the crank angle
$dQ_B/d\theta$	heat release rate with respect to the crank angle
$dQ_W/d\theta$	heat transfer rate to wall with respect to the crank angle
h_c	heat transfer coefficient (J/m^2 s K)
m	mass of cylinder gases (kg)
n_e	engine speed (r/min)
p	cylinder gas pressure (MPa)
p_{max}	maximum cylinder gas pressure (MPa)
p_{me}	brake mean effective pressure (MPa)
R	gas constant (J/kg K)
T	mean gas temperature (K)
T_{max}	maximum mean gas temperature (K)
T_w	wall temperature (K)
TDC	top dead centre
V	cylinder volume (m^3)
Δt_{injd}	fuel injection duration (ms)
$\Delta\theta_{fd}$	flame development duration (deg crank angle)
$\Delta\theta_{rd}$	rapid burning duration (deg crank angle)
$\Delta\theta_{td}$	total combustion duration(deg crank angle)
θ	crank angle (deg)
θ_c	crank angle of the centre of the heat release curve (deg crank angle after top dead centre)
θ_e	crank angle of the end of heat release (deg crank angle after top dead centre)
θ_{ign}	ignition advance angle (deg crank angle before top dead centre)
θ_{inj}	injection advance angle (deg crank angle before top dead centre)
θ_s	crank angle of the beginning of the heat release (deg crank angle before top dead centre)
λ	excess air ratio